JOURNAL OF AGRICULTURAL AND FOOD CHEMISTRY

Structural Investigations and Morphology of Tomato Fruit Starch

KIETSUDA LUENGWILAI AND DIANE M. BECKLES*

Department of Plant Sciences MS-3, University of California—Davis, 1 Peter Shields Avenue, Davis, California 95616

The physicochemical properties of starch from tomato (*Solanum lycopersicum* L.) pericarp and columella of cv. Moneymaker fruit at 28 days post anthesis (DPA) were investigated, providing the first description of the composition and structure of tomato fruit starch. Starch granules from pericarp were mainly polygonal, 13.5−14.3 μm, and increased in size through development, being largest in ripening fruit. Amylopectin content was 81−83% and was of molecular weight 1.01×10^8 g/mol; the phosphorus content was 139 ppm, and starch showed a C-type pattern with crystallinity of 30%. Starch characteristics were similar in columella except granule size (16.8−17.8 μm) and crystallinity (40%), although 6-fold more starch accumulated in the pericarp. Solara, a high-sugar tomato cultivar, was also studied to determine if this affects starch granule architecture. There were few differences from Moneymaker, except that Solara columella starch crystallinity was lower (26%), and more starch granule-intrinsic proteins could be extracted by sodium dodecyl sulfate−polyacrylamide gel electrophoresis.

KEYWORDS: Tomato fruit; starch biosynthesis; starch granule

INTRODUCTION

Tomato is one of the most economically valuable horticultural crops (*1*), and the soluble solids content in ripe fruit is a chief determinant of commercial value. Starch accumulation in green fruit may be one of many factors that contribute to the pool of sugars in ripe fruit (*2*), and as a result, the starch biosynthetic pathway has been studied as part of an effort to improve fruit quality (*3*−*5*). Unlike tubers stems and endosperm, tomato fruit starch is stored and degraded in one generation; it is typically synthesized in approximately 28 days and is then degraded over a subsequent 28 days as a source of carbon and energy in ripened fruit (*6*).

The composition and molecular structure of starch determine its physicochemical properties and are unique to the cellular conditions in which it was created. Starch is composed of polymerized glucose molecules organized into two types of α-1,4-glucans, amylose and amylopectin. Amylose is nearly linear with very few branches and typically accounts for 11−36% of starch weight among different species (*7, 8*). Amylopectin is a larger molecule of average molecular mass 10^7−10^9, and the α-1,4-glucan chains are branched every 20−30 glucose residues by α-1,6-linkages (*8*). These glucans are deposited to give rise to semicrystalline starch granules, which vary in shape, size, and composition depending on their botanical source and environment (*9*−*11*). Several studies also show that mutants and transgenic plants altered in carbohydrate metabolism often have altered starch granules (*11, 12*). This implies that the metabolic environment and starch biosynthetic enzymes present in the plastid are critical in shaping the starch granules made in a given tissue. Some starch biosynthetic enzymes can become entombed within the granule during biosynthesis, providing evidence of the activities that built the granule (*13*).

In this study, some of the physicochemical properties of tomato starch were investigated to discover its architecture and composition, as there are no published reports describing starch structure from this species. The specific questions that we wished to address are (i) what is the size, shape, and composition of tomato fruit starch granules and (ii) will these parameters differ between two cultivars that are drastically different in their fruit carbohydrate composition? There have been few explicit attempts to relate starch granule structure to its biosynthesis and subsequent degradation in fruit. Therefore, the properties of the starch granules produced in the two main starch-storing tissues of tomato, the pericarp and the columella, were studied. Work by others shows differences in carbohydrate metabolism between these tissues, and their anatomy is distinct (*4*). Two tomato cultivars were also examined that differ in carbohydrate metabolism. Solara is derived from a wild species, *Solanum pimpinellifolium* L., and accumulates twice the carbohydrates in the ripe fruit as compared to the standard research cultivar Moneymaker (*Solanum lycopersicum* L.). Comparison of starch from Moneymaker and Solara may reveal if differences in carbohydrate metabolism could potentially affect granule structures.

MATERIALS AND METHODS

Reagents and Plant Materials. All chemicals were purchased from Sigma-Aldrich (St. Louis, MO) unless otherwise stated. Seeds of *S. lycopersicum* L. cv. Moneymaker were obtained from the C.M. Rick Tomato Genetics Resource Center (Davis, CA). Seeds of *S.*

* To whom correspondence should be addressed. Tel: +1-530-754-4779. Fax: +1-530-752-9659. E-mail: dmbeckles@ucdavis.edu.

10.1021/jf802064w CCC: $40.75
Published on Web 12/18/2008

pimpinellifolium L. cv. Solara were a kind gift from Dr. Lilliana Stamova (Davis, CA).

Plant Growth Conditions. Tomato plants were grown in a greenhouse in Davis, CA, in standard soil media using 1.5 gallon pots. Fertilization was with 20−20−20 applied once per week during early growth and twice per week during flowering and fruit set. Supplemental lighting was provided to give a 16 h day. The average daily PAR light in the greenhouses was 25.25 ± 2.62 mol/m^{-2} s^{-1}. Temperatures averaged 18 °C at night and 25 °C during the day. Humidity was 50% (v/v) during the day and 90% (v/v) at night. All lateral branches were removed as they appeared to allow sufficient fruit set, enhanced plant health, and manageability.

Fruit Sampling. The fruit developmental stage was recorded by tagging flowers at pollination. For each study, six individual plants were used. Fruits were harvested at 14 and 28 days post anthesis (DPA), mature green and at breaker (when fruit was about to change the color), pink (*14*). Whole fruit was weighed, and 200−300 mg of fresh tissue was taken from the pericarp and columella of each fruit for starch measurement. The remainder of that fruit was used to determine dry weight by measuring the weight after 14 days of incubation in a ventilated oven at 55 °C.

Starch Measurements. The starch was determined using the method outlined in Beckles et al. (*15*). Samples were boiled in 80% (v/v) ethanol to remove soluble sugars. The ethanol-insoluble fraction was kept for starch measurement. Glucose released after enzymatic digestion of the ethanol insoluble fraction was measured by high-performance liquid chromatography (HPLC). Samples were injected onto a Hamilton RX-10 Anion exchange column (250 mm × 4.1 mm i.d.; Hamilton, Reno, NV), on a Dionex BioLC system (Dionex, Sunnyvale, CA) with pulse amperometric detection. The gradient elution schedule consisted of 15 min of 15% (v/v) of 200 mM NaOH, then 30% (v/v) of 200 mM NaOH over 7 min, and 15% (v/v) of 200 mM NaOH for 10 min. A standard solution of glucose (Fluka BioChemika Co.; Steinheim, Germany) was injected onto the column at a flow rate of 2.0 mL min^{-1}, and it eluted at 6.1 min. The starch content was calculated using the following equation: starch content = glucose content × (162/180).

Starch Granule Purification. *Method 1.* Fresh fruit was ground gently in 0.5 M NaCl, and the homogenate was filtered through a 175 μm mesh. The filtrate was resuspended by vortexing in 5 volumes of 0.5 M NaCl and was then centrifuged at 4000*g* for 10 min. The pellet was resuspended in 0.5 M NaCl and then recentrifuged. This step was repeated until most of the debris was removed. The pellet was then washed in water (three times), 2% (w/v) sodium dodecyl sulfate (SDS) (twice), water (12 times), and then once with 80% (v/v) acetone. The pellet was resuspended in 80% (v/v) acetone and allowed to settle, and the acetone was allowed to evaporate overnight until the starch was dried.

Method 2. Starch was also purified using a modification of the method from Forsyth et al. (*16*). Fresh fruit was homogenized in buffer containing 50 mM Tris-HCl, pH 8, 1 mM ethylenediaminetetraacetic acid (EDTA), 1 mM dithiothreitol (DTT), and 0.1% (w/v) sodium metabisulfite. The homogenate was filtered through four layers of miracloth, and the filtrate was centrifuged at 3220*g* for 5 min (*16*). The supernatant was discarded, and the pellet was resuspended in buffer and washed with 2% (w/v) SDS, water, and acetone as described in method 1.

Amylose Content. The amylose content was determined from three biological and two technical replicates using an amylose/amylopectin assay kit (K-AMYL, Megazyme International Ireland Ltd., Wicklow, Ireland). Starch was defatted and solubilized in DMSO, and the amylose was separated from amylopectin using concanavalin A.

Scanning Electron Microscope (SEM) and Light Microscopy of Starch. Purified starch was dusted onto carbon double stick discs (Pella, Redding CA), mounted onto 12 mm Aluminum stubs (Pella, Redding CA), and sputtered with gold on a BioRad Polaron sputter coater (model E51090). Particles were viewed under a FEI/Phillips XL30 SFEG SEM (Hillsboro, OR). Diameters of starch granules were estimated on the basis of the scale bar provided on the captured scanning electron micrographs. Light microscopy was performed using a Zeiss microscope (Oberkochen, Germany) with a 40× objective.

Starch Particle Size Analysis. Approximately 10−20 mg of purified starch was analyzed using the Microtec Analysette 22 (0.1−600 μm) Laser Scattering Particle Size Distribution Analyzer (Microtec, Laval, Quebec, Canada). The frequency of detection of granule of different sizes was recorded.

X-ray Powder Diffraction. X-ray powder diffraction of the purified starch was measured using a Scintag XDS 2000-ray diffractometer with XGEN4000 Scan Generator model (Scintag, Sunnyvale, CA). The operating conditions were a target current of 40 mA, filament of 3.23 Å, and power of 1.8 kW. The scanning range was 2−40°, and the scan speed was 0.02° per second. The degree of crystallinity was calculated by Origin8 software (OriginLab Corp., Northampton, MA) using the following equation: crystallinity (%) = $A_c/(A_c + A_a) \times 100$, where A_c = crystalline area and A_a = amorphous area on the X-ray diffractogram, respectively (*17*).

SDS−Polyacrylamide Gel Electrophoresis (PAGE) of Starch Granule Intrinsic Proteins. Batches of starch (40 mg) were dissolved in 800 μL of sample buffer containing 10% (w/v) SDS, 10% glycerol (v/v), 50 mM Tris-HCl (pH 8), and 100 mM DTT. The suspensions were boiled for 15 min with intermittent vortexing and cooled to room temperature. The supernatant was collected after centrifugation of the sample at 13000*g* for 15 min. The protein contained therein was precipitated by incubation in 4 volumes of acetone for 20 min at −20 °C followed by centrifugation at 13000*g* for 10 min at 4 °C. The protein was washed twice in 1 volume of cold 80% (v/v) acetone and then solubilized in 20 μL of buffer containing 50 mM Tris-HCl, pH 6.8, 10 mM EDTA, and 10 mM DTT. Approximately 6.5 μL of sample was loaded onto 12% (w/v) precast Bis-Tris SDS-PAGE gel (Invitrogen, Carlsbad, CA). Sypro Ruby (Molecular Probe, Invitrogen) was used to stain the separated proteins, which were visualized by UV light at 260 nm using an AlphaImager (Alpha Innotech, San Leandro, CA).

Phosphate and Total Phosphorus. Total extractable phosphate was determined using the method outlined in Prokopy (*18*). *ortho*-Phosphate (PO_4-P) was extracted from 50 mg of tomato starch using 2% (v/v) acetic acid and was then determined spectrophotometrically at 660 nm by reacting with paramolybdate using an automated flow injection analyzer (FIA).

Total phosphorus was quantitatively determined from 250 mg of starch. The sample was subjected to nitric acid/hydrogen peroxide microwave digestion, and total phosphorus was determined by atomic absorption spectrometry (AAS) and inductively coupled plasma atomic emission spectrometry (ICP-AES) (*19*).

High-Performance Size-Exclusion Chromatography (HPSEC)−Multiangle Laser Light Scattering Detector (MALLS)-RI System for Molecular Weight Determination. The HPSEC system consisted of an HP 1050 series pump and autoinjector (Hewlett-Packard, Valley Forge, PA) fitted with a 100 μL injection loop. The system also employed a MALLS (Dawn DSP-F, Wyatt Tech., Santa Barbara, CA) with He−Ne laser source (λ = 632.8 nm), a k-5 flow cell, and a differential refractometer detector (RI) (model ERC-7512, ERMA Inc., Tokyo, Japan).

HPSEC Analysis of Tomato Starch Molecular Mass. Starch was prepared following the method by Yokoyama et al. with minor modifications (*20*). Starch was added to 50 mM LiBr in DMSO at 0.4% (w/v) and then heated at 95 °C for 15 min with constant stirring. The samples were cooled and continuously stirred overnight and then centrifuged for 10 min at 3220*g*. The supernatant was filtered through a 1.2 μm nylon syringe membrane filter and analyzed with the HPSEC system.

Two different mobile phases and column banks were used for the determination of the molecular weight distributions. A bank of Waters Stragel columns (HMW 6E, 6E, and 2) was used with 50 mM LiBr (Fisher Scientific, Fair Lawn, NJ) in DMSO (HPLC grade) with 50 mM LiBr as a mobile phase with a flow rate of 0.4 mL/min. The refractive index of 1.479 and the d*n*/d*c* value of 0.066 for starch in DMSO/50 mM LiBr were used for the molecular weight calculations.

Enzymatic Debranching of Tomato Fruit Starch. Moneymaker tomato starch was debranched using the method outlined in Bradbury and Bello (*21*) and Ward, et al. (*22*) with some modifications. The starch samples (50 mg) were solubilized by heating at 95 °C for 15

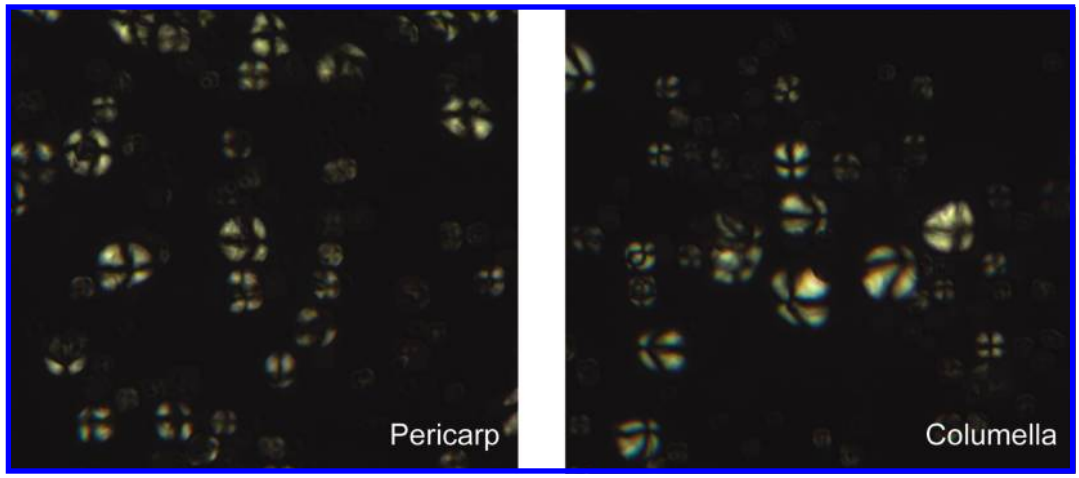

Figure 1. Light microscopy of iodine-stained starch under polarized light. Starch was purified from pericarp and columella tissue at 28 DPA from the Moneymaker tomato cultivar. The typical maltese cross was observed, indicating intact starch granules. Magnification, 40×.

min in 5 mL of distilled water. The tubes were then cooled down to 45 °C for 5 min. After cooling, samples were digested with isoamylase (42 U per mg of starch) from *Pseudomonas* spp. in 5 mL of 40 mM acetate buffer (pH 3.8). After 24 h, the reaction was stopped by heating the tube for 10 min at 100 °C. The debranched solution was centrifuged, and the supernatant was filtered through a 0.2 μm nylon syringe membrane filter (*21*, *22*). The filtrate was then analyzed to determine the averaged molecular weights (M_w) of amylopectin branches using a two HPSEC column (Ultragel 1000 and Ultragel 250) with 0.1 N $NaNO_3$ as the eluent. The HPSEC system was operated as described above. The analysis was performed using six biological replicates.

Statistical Analysis. Statistical analyses were determined by Student's *t* test using Microsoft Excel (2003). Data were considered statistical significant if $P < 0.05$.

RESULTS AND DISCUSSION

Tomato Starch Granule Morphology and Composition. In this study, we wished to investigate the chemical and physical properties that help shape starch granule architecture in tomato fruit. The pericarp and especially the columella are the primary sites of starch storage in immature tomato fruit (*4*, *6*); thus, these two tissues were examined in *S. lycopersicum* L. cv. Moneymaker.

Starch Granule Morphology. Tomato starch granule morphology was assessed to determine the extent to which it changed, if at all, during development by light microscopy and SEM (**Figures 1**−**3**). When viewed under polarized light, starch granules showed the characteristic birefringence or maltese cross, indicating that the isolation method used yielded largely intact, native starch granules (*23*) (**Figure 1**). Tomato starch granules varied in shape with most being spherical and polygonal, although some dome-shaped starch granules were observed (**Figure 2**). It is possible that some of the granules might have been damaged during purification. Similar morphologies were reported for starches isolated from pineapple stem, pejibaye fruit, and acorn kernels (*24*). Irregular surface indentations, including smooth undulating ridges and, occasionally, concentric peeling and rivulets, were also evident in granules from both tissues (**Figures 2** and **3**). While it is possible that these surface indentations are due to rapid enzymatic degradation during in vitro extraction, this seems unlikely. Starch was extracted within an hour from freshly harvested fruit using buffer-containing reagents to inhibit proteolytic degradation. It is possible that these surface indentations are characteristic of tomato fruit starch granules. "Pin-holes" were also evident on the surface of some granules at each developmental stage examined (**Figure 3**). "Pin-holes" are usually seen in cereal starches undergoing enzymatic hydrolysis during germination, and the occurrence of these "pin-holes" in tomato starch, especially during the period of active starch synthesis (14 DPA), could suggest that hydrolysis and by extension, turnover, of starch occurs in developing tomato fruit (*25*).

Evidence from in vitro studies indicates that starch granule size can affect the rate of its degradation (*26*, *27*). Therefore, granule size may influence the rate of starch breakdown and hence, substrate availability in ripening tomato fruit. Tomato fruit granule size was estimated using SEM and laser scattering. Starch granules ranged from 10 to 25 μm at all developmental stages and in all tissues examined (**Figure 2** and **Table 1**). Laser diffraction was used to estimate the mean, mode, and starch particle size distribution in a larger granule population (**Figures 4** and **5**). Laser diffraction is not a precise method of measuring granule size as it assumes that all granules are spherical, which was not true of our sample. However, it permits granule size estimation of a very large population not possibly determined by eye (*28*). Two classes of tomato starch granule size were observed, which changed during fruit development. The small-granule class found at the immature stage gradually decreased at later stages (**Figure 4**). There are three possibilities to potentially explain this: (i) There was a single round of granule initiation, and most granules increased in size during fruit development, thereby reducing the proportion of the small-sized granule class detected; (ii) during fruit maturation, the small granules were degraded preferentially reducing their contribution to particle size distribution; or (iii) some of the granules, including the small ones, fused together, forming aggregates of a larger size. These explanations are not mutually exclusive, and these three processes may occur to varying degrees at a given time.

Starch granule size increased, albeit slightly, as fruit growth progressed to maturation over the 42 days examined (**Figures 2**, **4**, and **5**). The increase in granule size occurred even during the phase of net starch degradation when fruits were at the pink stage (**Figure 2**). The fact that the granule exterior surface remained intact even at the pink stage suggests that starch granule degradation might start from the "inside out" in tomato as found in starch from yam tubers (*10*) and water caltrop fruit starch (*9*). "Inside-out" digestion describes the mode of starch digestion that is initiated in the core of the granule and proceeds outward, leaving the outer shell intact while the granule becomes hollow (*29*). However, on some granules, concentric peeling—

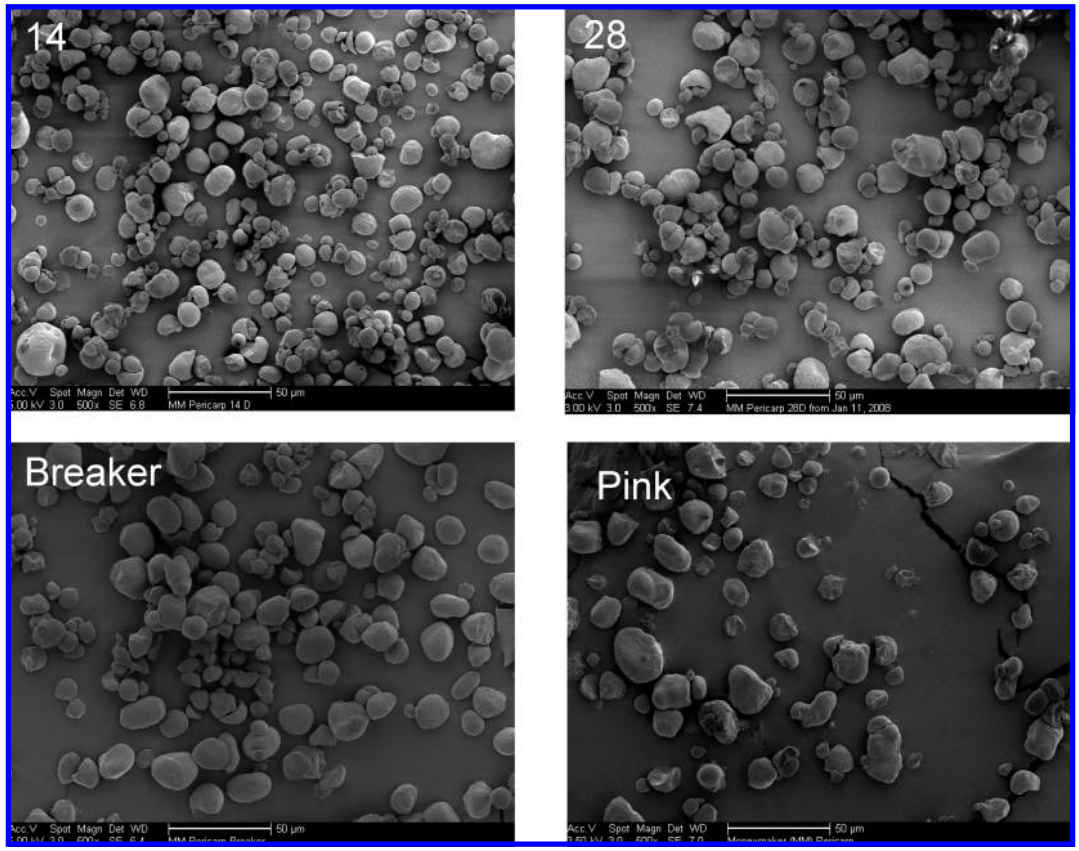

Figure 2. Scanning electron micrographs of starch purified from Moneymaker tomato fruit. Starch was purified from pericarp tissue at 14 and 28 DPA, Breaker and Pink stage. Granules varied in shape from spherical to polygonal with some dome-shaped and irregularly shaped. Starch granule size increased slightly as fruit development proceeded. Magnification was 500×, and scale bar = 50 μm.

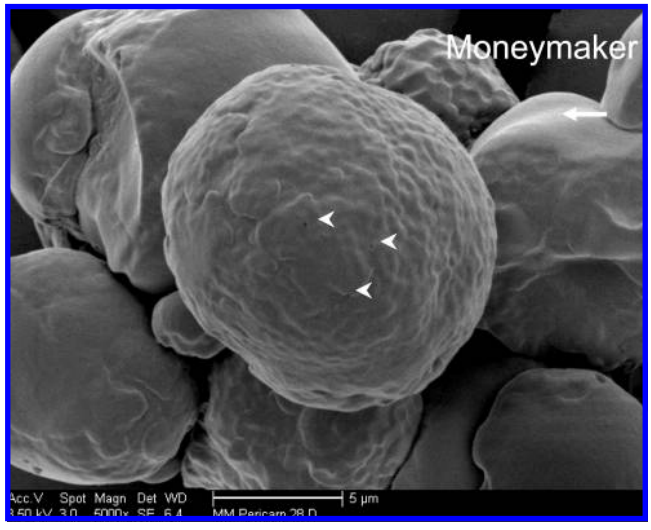

Figure 3. Scanning electron micrographs of starch purified from Moneymaker tomato fruit. Starch was purified from pericarp tissue at 28 DPA. Pin-holes (arrowhead) and concentric peeling (arrow) were evident on the surface of granules. Magnification was 5000×, and scale bar = 5 μm.

indicative of exo-corrosion—was detected, so the mechanism of tomato starch granule degradation is still unclear.

Granule sizes differed between columella and pericarp at the same physiological stage (**Table 1**, **Figure 5**, and data not shown) and were slightly larger in the columella (16.8−17.8 μm) than in the pericarp (13.5−14.3 μm). At most stages examined, tomato starch granules are also larger relative to other fruit starch, where it has been measured [e.g., mango (5−10 μm, *30*); pineapple (3−10 μm, *24*); and apple (2−12 μm, *31*)]. The largest modal granule size recorded was >25 μm from pink-fruit columella, which is relatively the same modal size as the large A type granules of wheat and rye endosperm starch at grain maturity (*24*).

Table 1. Structural Characteristics of Tomato Starch at 28 DPA[a]

starch composition	Moneymaker
starch granule size in pericarp, mode (μm)	13.9 ± 0.4[b]
starch granule size in columella, mode (μm)	17.3 ± 0.5[b]
amylose content in pericarp (%)	18.4 ± 0.7
amylose content in columella (%)	16.5 ± 0.6
degree of crystallinity in pericarp (%)	30.7 ± 3.8[b]
degree of crystallinity in columella (%)	40.1 ± 4.7[b]
total extractable phosphate (ppm)	<10.0 ± 0.0
total phosphorus at mature green stage (ppm)	139.0 ± 6.3
amylopectin molecular weight in pericarp (g/mol)	1.01 × 10^8

[a] Starch granule size was estimated using laser diffraction. The amylose content was determined using an amylose/amylopectin assay kit (K-AMYL). The degree of crystallinity was calculated from X-ray powder diffraction (**Figure 6**). The total extractable phosphate was analyzed by a FIA, and total phosphorus was determined by AAS and ICP-AES. The amylopectin molecular weight was assayed from pericarp tissue using a HPSEC system. Values are the mean ± standard error of mean (*N* = three biological replicates; unless otherwise stated). Note: Total phosphate was measured in starch from mature green fruit; however, data were the same in two measurements at 28 DPA. The amylopectin molecular weight of pericarp starch was measured from two biological replicates. [b] Data were significantly different at $P < 0.05$.

Amylopectin-to-Amylose Ratio. The proportion of amylopectin to amylose of tomato starch was assayed as this may affect the rate at which starch is hydrolyzed to sugars—through the ratio itself or how it affects starch organization (*26*, *32*). Starches with amylopectin contents ranging from 70 to 83% may be

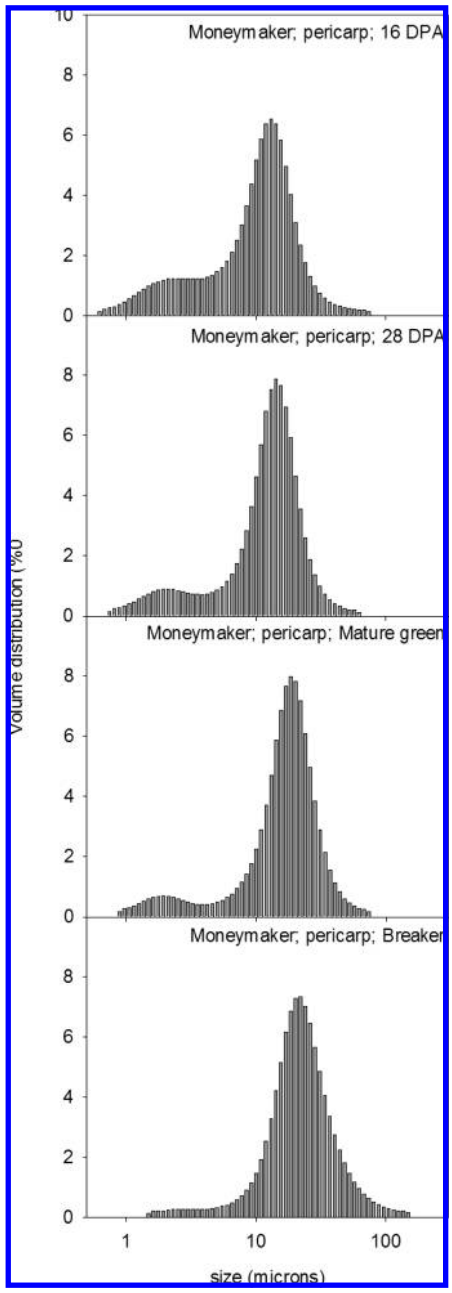

Figure 4. Starch particle size distribution of Moneymaker by laser diffraction. Starch was purified from pericarp at 16 and 28 DPA, mature green and breaker stage. The data showed that the proportion of smaller granules (less than 10 μm) decreased as the fruit matured.

classified as normal and can be found in primary starch-storing organs of squash, corn, rice, wheat, and potato (*33, 34*). We found that the amylose content in tomato fruit starch was 16.5−18.4% for both starch-synthesizing tissues at 28 DPA (**Table 1**). These values are similar to those found in banana starch [16−19% (*35*−*38*)] but much lower than that reported for apple [26−29% (*24*)]. The amylopectin content of tomato starch (81.6−83.5%) is therefore to the higher end of the normal range.

Phosphate Content. The phosphorus content of potato tuber starch is high (308−1244 ppm) and has been found to have a direct correlation with starch degradability in that organ (*39*). Therefore, we wished to determine the phosphorus content of tomato starch to assess whether it could influence the starch degradation during ripening. The total phosphorus content of Moneymaker tomato starch at mature green stage was 139 ppm with less than 10 ppm of total extractable phosphate (**Table 1**). The tomato starch phosphorus content is much less than that in potatoes but is in the same range as that of most other species (*40*). This result indicated that phosphorus might not have a great role in tomato starch degradation as compared to potato.

Crystalline Structure and Degree of Crystallinity. The starch crystalline structure is described as either A, B, or C depending on the packing of the amylopectin side chain into double helices. Unlike A-type starches, which have tightly packed double helices, B-type starches have a more open packing of helices with more interhelical water. Differences in susceptibility to enzymatic hydrolysis between the A- and the B-type may therefore be expected. Cereal starches have an A- type structure, tubers have a B type structure, while legumes, tropical tubers, apple, and banana fruit starches are a mixture of A and B crystallites and are described as C-type starches (*8, 11, 41*). It appears that a range of crystalline structures can be found in the starch-storing tissues of different cultivars, for example, in banana, A-, B-, and C-type crystalline structures have been reported (*38*). X-ray powder diffraction was used to observe the arrangement of the glucan chains of tomato starch. The X-ray crystallogram of 28 DPA starch from both tissues showed the strongest diffraction peak at 17.2° 2θ and a few small peaks at around 2θ of values 5.5, 15.4, 20, 22.8, and 23.6° were evident (**Figure 6**). Thus, the tomato starches that we studied are indicative of a C-type X-ray pattern (*8, 42*). The degree of crystallinity was 40.1 and 30.7% in columella and pericarp tissue, respectively (**Table 2**). Starch crystallinity values range from 20 to 45% for several starches [e.g., 40−47% in apple (*24*) and 21% in mango starch (*43*)]; therefore, tomato starch, especially from the pericarp, is toward the high of this range (*42, 44*).

M_w of Starch from Pericarp. The molecular weight of pericarp starch amylopectin at 28 DPA was determined by HPSEC (**Figure 7**). The chromatogram showed a high molecular weight peak of the amylopectin fraction with the concentration maxima at elution volume (V_e) equal to 17.2 mL. The M_w of amylopectin from this starch was determined to be 1.01×10^8 g/mol, and the *z*-averaged mean square radius (rms) was 199.3 nm. These values were comparable to rice (0.5×10^8 g/mol), barley (1.3×10^8 g/mol), potato (1.7×10^8 g/mol), lotus root (1.5×10^8 g/mol), and green banana starch [1.9×10^8 g/mol (*45*−*47*)] but smaller than apple starch [$4.6-11.1 \times 10^8$ g/mol (*31*)].

Distribution of Branch Chain Length in Amylopectin of Columella and Pericarp Starch. Amylopectin molecular weight distribution is believed to be important in determining the extent and nature of the crystallinity of the granule, which, in turn, influences granule morphology (*11, 48, 49*). Amylopectin molecular weight also correlates with glucan chain distribution, and the latter may be estimated by examining the distribution of amylopectin molecular weight after enzymatic debranching of starch. The HPSEC and MALLS with RI system has been commonly used to analyze glucan chains produced after starch has been debranched (*45*). This method provides a broad description of all of the resultant chains in the debranched starch dispersion from which glucan chain distribution may be inferred. The output is described in terms of the refraction produced by the volume of the glucan eluted from the column. You and Izydorczyk found an inverse correlation between amylopectin molecular weight and amylose content (*50*).

The debranched starches of Moneymaker tomato fruit at mature green were separated into two major peak fractions, attributed to high molecular weight linear amylose fraction (5−8

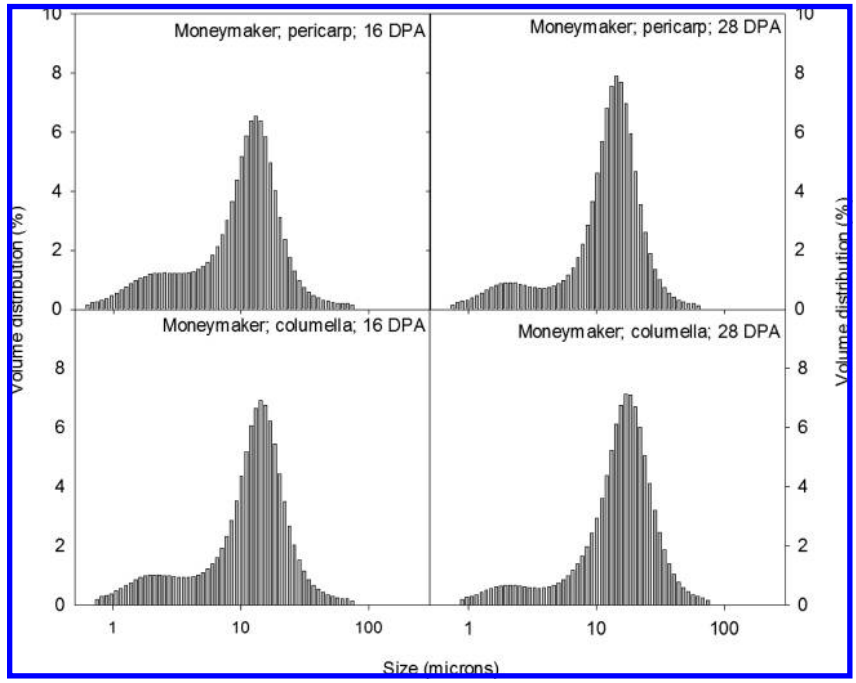

Figure 5. Starch particle size distribution of Moneymaker by laser diffraction. Starch was purified from pericarp and columella at 16 and 28 DPA. Approximately 10 mg of purified starch was analyzed. The data showed the frequency of occurrence of granules of a particular size based on volume.

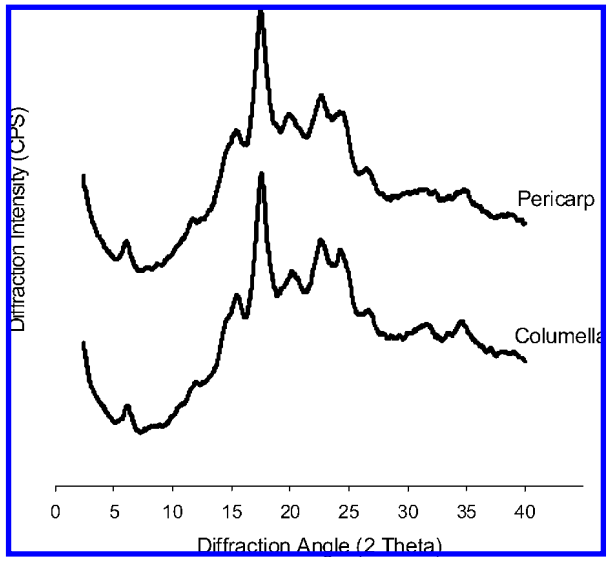

Figure 6. X-ray powder diffractogram of starch purified from pericarp and columella of Moneymaker at 28 DPA using a Scintag X-ray diffractometer.

mL of elution volume; not shown) and two peaks representing a fraction of lower molecular weight linear amylopectin eluting at ~15 and ~17 mL (**Figure 8**). The molecular weights of the amylopectin fraction of Moneymaker pericarp and columella were $2.5 \pm 0.4 \times 10^4$ and $4.9 \pm 2.1 \times 10^4$ g/mol, respectively. Perhaps because of the high variability in columella tissue, no significant difference between these samples was found.

Overall, the parameters assayed and measured for tomato starch fall within the range of that measured for other species. Amylopectin content (81−83%) and crystallinity (30.7−40.1%), however, are toward the high end of the known range for starches. From a naive perspective, it may be expected that several structural features of tomato starch would be intermediate to that of leaf and storage starches starch, given that the period of synthesis is rather short, and in the tomato lines that we studied, net degradation is detected as early as 21 DPA (data not shown). In theory, smaller granules (modal class 10−12 μm) and starch with a high proportion of amylopectin and high phosphate content would support a rapid rate of hydrolysis. Of these characteristics, only amylopectin content was found to be consistent with our expectations. Furthermore, the size of the granules in mature fruit (25 μm) was comparable to that of some cereals, although the period of synthesis is much reduced. In addition, we observed no significant differences between starch purified from the pericarp vs that from the columella except granule size and degree of crystallinity, although carbohydrate metabolism and morphology of these tissues are distinct (*4*, *51*).

Tomato starch granules appear to increase in size through development, even during the period of net degradation, indicating that synthesis and degradation may be occurring simultaneously. Starch hydrolytic and phosphorolytic enzymes are present in the plastid early in development (*15*, *52*), and simultaneous synthesis and degradation in tomato fruit were proposed in another study (*25*), making this possible. We also observed pinholes on the surface of several granules isolated from developing fruit, which further support the hydrolysis hypothesis. However, to determine if appreciable turnover of starch occurs in developing tomato fruit would require further investigation.

Starch Content and Some Structural Characteristics of Two Tomato Cultivars Differing in Carbohydrate Metabolism. *Starch Content.* To learn more about how granule characteristics may be potentially influenced by carbohydrate metabolism, we compared a number of biochemical and starch analytical features of Moneymaker to that of a high sugar tomato cultivar Solara, which has high total soluble solids content in the ripe fruit (unpublished data). A higher proportion and total amount of starch in young fruit might potentially explain the higher sugar in Solara as compared to Moneymaker (*4*). More importantly, it provides an opportunity to determine if the difference in carbohydrate metabolism can affect starch granule structure.

Table 2. Tomato Starch Granule Size, Amylose Content, and Crystalline Structure Pattern[a]

tissue	cultivar	starch granule size (μm)	amylose content (%)	degree of crystallinity (%)	crystalline structure type
pericarp	Moneymaker	13.9 ± 1.1	18.4 ± 2.9	30.7 ± 3.8	C
	Solara	14.9 ± 2.1	19.1 ± 1.4	N/A	C
columella	Moneymaker	17.3 ± 1.2	16.5 ± 2.6	40.1 ± 4.7[b]	C
	Solara	18.5 ± 2.2	17.4 ± 1.6	26.1 ± 3.9[b]	C

[a] Starch was purified from Moneymaker and Solara fruit at 28 DPA. Note: N/A = data were not available. [b] Data were significantly different at $P < 0.05$.

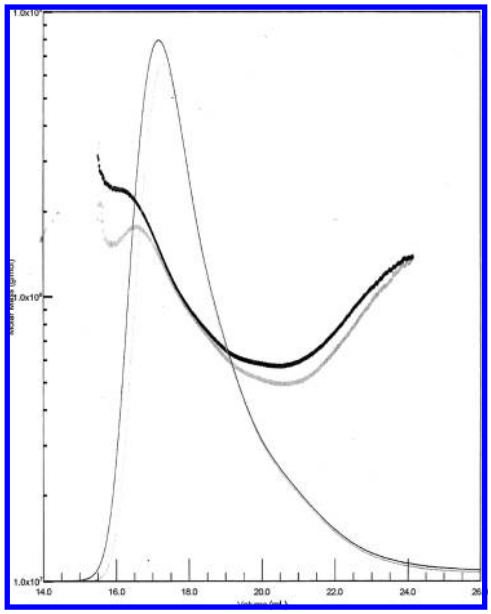

Figure 7. HPSEC profiles of amylopectin molecular weight of Moneymaker starch. Starch was dispersed in DMSO at 0.4% (w/v), heated at 95 °C for 15 min, and then continuously stirred for 24 h at room temperature. The supernatant was analyzed with the HPSEC system. The amylopectin molecular weight distribution (thin line) and the RI signal profile (thick line) are shown. The chromatogram showed the duplicated measurement of the same sample.

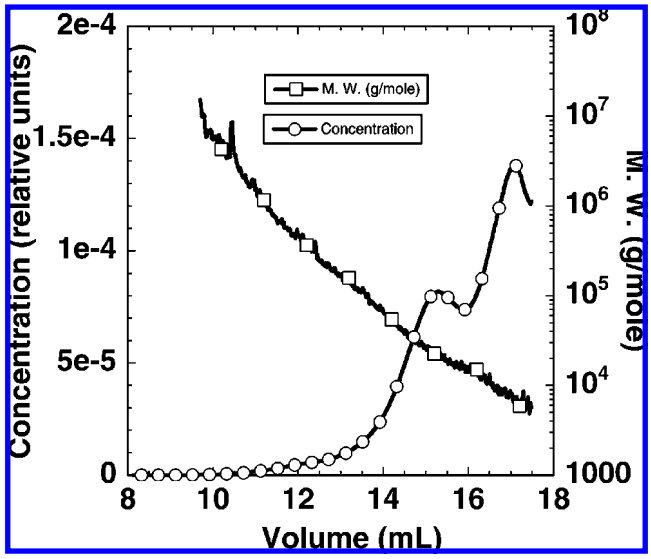

Figure 8. Elution profile of debranched starch. Starch from mature green stage was debranched by isoamylase. The debranched starch was then measured by two HPSEC columns using 0.1 N $NaNO_3$ as the eluent at a flow rate of 0.6 mL/min.

To estimate the total amount of starch accumulated in each fruit, the whole fruit was weighed, and then, the pericarp and columella fractions were separated and weighed individually and starch was determined in each. This was done for fruit from both genotypes at 28 DPA. At 28 DPA, Moneymaker fruit was almost twice the mass of Solara and accumulated 43% more starch per fruit (**Figure 9**). There was 6-fold more starch accumulated in Moneymaker pericarp as compared to the columella when considered on a dry weight basis, whereas starch was partitioned equally in both columella and pericarp in Solara. From these data, it would appear that starch metabolism is different between cultivars with significantly more accumulated at 28 DPA in Moneymaker than in Solara. There may therefore be greater biosynthesis of starch in Moneymaker and/or more degradation of starch in Solara at equivalent stages. Starch accumulation and metabolism in pericarp and columella may thus be sufficiently different in these two cultivars to investigate if fruit metabolism affects starch granule characteristics.

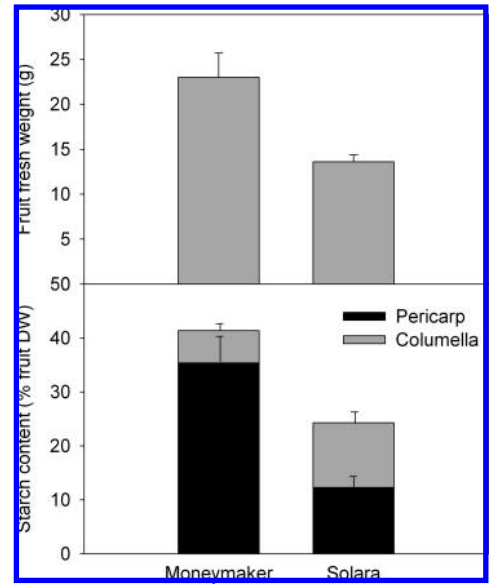

Figure 9. Fruit fresh weight (fruit mass) and starch content of Moneymaker and Solara fruit. The whole fruit at 28 DPA was weighed, and the starch-storing portion represented by the pericarp and columella was excised from the gelatinous fraction, which was discarded. The mass of each tissue type was determined and recorded. Values are the means ± SEM of 6−12 fruits.

Starch Structural Characteristics. We compared Solara tomato starch granule morphology from both pericarp and columella at 14, 28, 35 and breaker to equivalent stages in Moneymaker. Spherical and polygonal granules ranging from 11 to 19 μm were also observed in Solara, and as in Moneymaker, granules increased in size throughout development (data not shown). The amylose contents measured from both cultivars were between 17 and 20% at 28 DPA and were not significantly different. Similar to Moneymaker starch, Solara starch had a C-type X-ray diffraction pattern. However, the degree of crystallinity in columella tissue of Solara was significantly less than that in Moneymaker (**Table 2**). While these two tomato genotypes showed no difference in starch granule structure and composition, there is evidence (from the crystallinity data) that

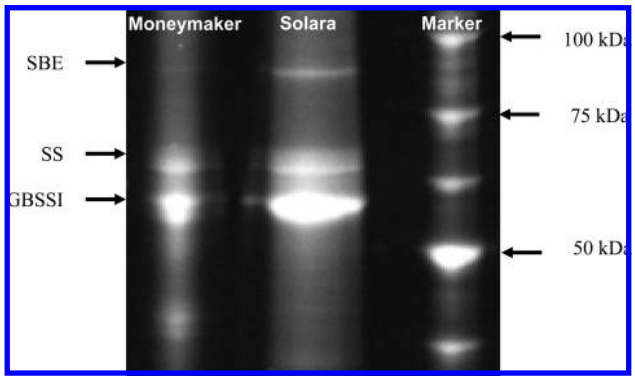

Figure 10. Starch granule-bound proteins in columella of Moneymaker and Solara in mature green fruit. Starch (40 mg) was gelatinized in SDS buffer at 100 °C, and proteins were extracted by centrifugation. Extracted proteins were concentrated and run on a 12% SDS-PAGE. The separated proteins were visualized by staining the gel with Sypro Ruby, and the image was captured under UV light using the Alphalmager. The bands shown are predicted to be granule-bound starch synthase I (60 kDa), starch synthase (70 kDa), and starch branching enzyme (85 kDa) based on their gel mobility as compared to the known molecular mass of these proteins. The amount of protein in pericarp was below the level that could be reliably detected by SDS-PAGE.

disparities in fine molecular structure may exist. Therefore, further studies of the thermal properties, degree of polymerization of glucan chains, and structural investigations by NMR, atomic force microscopy, and both short- and wide-angle diffraction of these starches may be needed to fully understand the extent to which they are similar.

SDS-PAGE of Starch Granule-Bound Proteins. The proteins that directly build up the starch granules are often entombed within the granule and leave behind evidence of the activities that are involved in its synthesis (*53*−*55*). If the starch-storing tissue of the two tomato cultivars accumulated different amounts of starch, it might be partly due to the different complement of starch biosynthetic proteins present in the plastid. Differences in the protein profile between cultivars could be reflected in the starch granule-associated proteins (SGAPs). To test this, an equal amount of purified starch granules from Moneymaker and Solara columella at the mature green stage was gelatinized in SDS buffer, and the extracted SGAPs were loaded onto SDS-PAGE gels for analysis. Three protein bands of molecular mass 60, 70, and 85 kDa were seen (**Figure 10**). On the basis of their mobility through SDS-PAGE gels and comparison with published work, these bands were putatively identified as GBSS I (granule-bound starch synthase I; 60 kDa), SS (starch synthase; 70 kDa), and SBE (starch branching enzyme; 85 kDa) (*53*, *55*−*59*). This result was typically observed in three gels from three different batches of starch prepared from separate fruits. More protein could be extracted from Solara columella starch than from Moneymaker. This may reflect differences in the total protein found associated with the starch granule or differences in protein extractability due to the structural features of the respective starches. However, more starch accumulated in Solara columella, and in accordance, more SGAPs were found in this tissue when compared to Moneymaker, which may be indicative of real differences in metabolism. The disparity in SGAPs might be one of the contributing factors that result in the different metabolic events between these two cultivars.

In conclusion, some molecular features of tomato fruit starches from two cultivars were investigated to first discover the nature of starch in this organ and then to gain insight into whether its synthesis can be influenced by metabolic events in the cell and/or, in turn, if its structure may influence subsequent metabolism. Overall, the parameters assayed and measured in tomato starch from both genotypes showed no significant differences in granule morphology, amylose content, X-ray diffraction type at any stage, or tissue between the two cultivars as observed except the degree of crystallinity in columella tissue. This is perhaps surprising since Moneymaker fruit accumulates 43% more starch, stores most of it in the pericarp, and less GBSSI, SS, and SBE proteins could be extracted from its columella starch as compared to Solara. This result suggests that the components of carbohydrate metabolism, which shape starch granule biosynthesis in tomato fruit, are similar in these two genotypes, producing granules of identical size, shape, and composition. However, other components of carbohydrate metabolism also exist that lead to large differences in the total amount of starch synthesized.

ACKNOWLEDGMENT

We thank Dr. Charles Shoemaker, Department Food Sciences, UC Davis, for amylopectin molecular mass and polydispersity measurements, Pamela Chacha, Lisa Zhao, and Eric Lau for technical assistance, and Dr. Kanitha Tananuwong for critical reading of the manuscript.

LITERATURE CITED

(1) U.S. Department of Agriculture. Tomatoes. Tomatoes at a Glance; Economic Research Service: Washington, DC, 2008.

(2) Schaffer, A. A.; Levin, I.; Oguz, I.; Petreikov, M.; Cincarevsky, F.; Yeselson, Y.; Shen, S.; Gilboa, N.; Bar, M. ADPglucose pyrophosphorylase activity and starch accumulation in immature tomato fruit: The effect of a *Lycopersicon hirsutum*-derived introgression encoding for the large subunit. *Plant Sci*. **2000**, *152* (2), 135–144.

(3) Petreikov, M.; Shen, S.; Yeselson, Y.; Levin, I.; Bar, M.; Schaffer, A. A. Temporally extended gene expression of the ADP-Glc pyrophosphorylase large subunit (AgpL1) leads to increased enzyme activity in developing tomato fruit. *Planta* **2006**, *224* (6), 1465–1479.

(4) Schaffer, A. A.; Petreikov, M. Sucrose-to-starch metabolism in tomato fruit undergoing transient starch accumulation. *Plant Physiol*. **1997**, *113* (3), 739–746.

(5) Dinar, M.; Stevens, M. A. The relationship between starch accumulation and soluble solids content of tomato fruits. *J. Am. Soc. Hortic. Sci*. **1981**, *106* (4), 415–418.

(6) Obiadalla-Ali, H.; Fernie, A. R.; Kossmann, J.; Lloyd, J. R. Developmental analysis of carbohydrate metabolism in tomato (*Lycopersicon esculentum* cv. Micro-Tom) fruits. *Physiol. Plant*. **2004**, *120* (2), 196–204.

(7) Detherage, W. L.; MacMasters, M. M.; Rist, C. E. A partial survey of amylose content in starch from domestic and foreign varieties of corn, wheat, and sorghum and from some other starchbearing plants. *Trans. Am. Assoc. Cereal Chem.* **1955**, *13*, 31–42.

(8) Tester, R. F.; Karkalas, J.; Qi, X. Starch—Composition, fine structure and architecture. *J. Cereal Sci*. **2004**, *39* (2), 151–165.

(9) Chiang, P. Y.; Li, P. H.; Huang, C. C.; Wang, C. C. R. Changes in functional characteristics of starch during water caltrop (*Trapa Quadrispinosa* Roxb.) growth. *Food Chem*. **2007**, *104* (1), 376–382.

(10) Huang, C. C.; Lin, M. C.; Wang, C. C. R. Changes in morphological, thermal and pasting properties of yam (*Dioscorea alata*) starch during growth. *Carbohydr. Polym*. **2006**, *64* (4), 524–531.

(11) Buleon, A.; Colonna, P.; Planchot, V.; Ball, S. Starch granules: Structure and biosynthesis. *Int. J. Biol. Macromol*. **1998**, *23* (2), 85–112.

(12) Roldan, I.; Wattebled, F.; Lucas, M. M.; Delvalle, D.; Planchot, V.; Jimenez, S.; Perez, R.; Ball, S.; D'Hulst, C.; Merida, A. The phenotype of soluble starch synthase IV defective mutants of *Arabidopsis thaliana* suggests a novel function of elongation enzymes in the control of starch granule formation. *Plant J.* **2007**, *49* (3), 492–504.
(13) Baldwin, P. M. Starch granule-associated proteins and polypeptides: A review. *Starch-Starke* **2001**, *53* (10), 475–503.
(14) U.S. Department of Agriculture. USDA Standard for Grades of Fresh Tomatoes; U.S. Department of Agriculture: Washington, DC, 1997.
(15) Beckles, D. M.; Craig, J.; Smith, A. M. ADP-glucose pyrophosphorylase is located in the plastid in developing tomato fruit. *Plant Physiol.* **2001**, *126* (1), 261–266.
(16) Forsyth, J. L.; Ring, S. G.; Noel, T. R.; Parker, R.; Cairns, P.; Findlay, K.; Shewry, P. R. Characterization of starch from tubers of yam bean (*Pachyrhizus ahipa*). *J. Agric. Food Chem.* **2002**, *50* (2), 361–367.
(17) Shujun, W.; Jinglin, Y.; Wenyuan, G. Use of X-ray diffractometry (XRD) for identification of Fritillaria according to geographical origin. *Am. J. Biochem. Biotechnol.* **2005**, *1* (4), 207–211.
(18) Prokopy, W. R. Phosphorus in acetic acid extracts. In *QuikChem Method 12-115-01-1-C*; Lachat Instruments: Milwaukee, WI, 1995.
(19) Sah, R. N.; Miller, R. O. Spontaneous reaction for acid dissolution of biological tissues in closed vessels. *Anal. Chem.* **1992**, *64*, 230–233.
(20) Yokoyama, W.; Renner-Nantz, J. J.; Shoemaker, C. F. Starch molecular mass and size by size-exclusion chromatography in DMSO-LiBr coupled with multiple angle laser light scattering. *Cereal Chem.* **1998**, *75* (4), 530–535.
(21) Bradbury, A. G. W.; Bello, A. B. T. Determination of molecular-size distribution of starch and debranched starch by a single procedure using high-performance size-exclusion chromatography. *Cereal Chem.* **1993**, *70* (5), 543–547.
(22) Ward, K. E. J.; Hoseney, R. C.; Seib, P. A. Retrogradation of amylopectin from maize and wheat starches. *Cereal Chem.* **1994**, *71* (2), 150–155.
(23) Millan-Testa, C. E.; Mendez-Montealvo, M. G.; Ottenhof, M. A.; Farhat, I. A.; Bello-Perez, L. A. Determination of the molecular and structural characteristics of Okenia, Mango, and banana starches. *J. Agric. Food Chem.* **2005**, *53* (3), 495–501.
(24) Jane, J. L.; Kasemsuwan, T.; Leas, S.; Zobel, H.; Robyt, J. F. Anthology of starch granule morphology by scanning electron-microscopy. *Starch-Starke* **1994**, *46* (4), 121–129.
(25) N'tchobo, H.; Dali, N.; Nguyen-Quoc, B.; Foyer, C. H.; Yelle, S. Starch synthesis in tomato remains constant throughout fruit development and is dependent on sucrose supply and sucrose synthase activity. *J. Exp. Bot.* **1999**, *50* (338), 1457–1463.
(26) Svihus, B.; Uhlen, A. K.; Harstad, O. M. Effect of starch granule structure, associated components and processing on nutritive value of cereal starch: A review. *Anim. Feed Sci. Technol.* **2005**, *122* (3−4), 303–320.
(27) Tamaki, S.; Teranishi, K.; Hisamatsu, M.; Yamada, T. Inner structure of potato starch granules. *Starch-Starke* **1997**, *49* (10), 387–390.
(28) Wilson, J. D.; Bechtel, D. B.; Todd, T. C.; Seib, P. A. Measurement of wheat starch granule size distribution using image analysis and laser diffraction technology. *Cereal Chem.* **2006**, *83* (3), 259–268.
(29) Hallett, I. C.; Wegrzyn, T. F.; Macrae, E. A. Starch degradation in kiwifruit—In-vivo and in-vitro ultrastructural studies. *Int. J. Plant Sci.* **1995**, *156* (4), 471–480.
(30) Bello-Perez, L. A.; Aparicio-Saguilan, A.; Mendez-Montealvo, G.; Solorza-Feria, J.; Flores-Huicochea, E. Isolation and partial characterization of mango (*Magnifera indica* L.) starch: Morphological, physicochemical and functional studies. *Plant Foods Hum. Nutr.* **2005**, *60* (1), 7–12.
(31) Stevenson, D. G.; Domoto, P. A.; Jane, J. L. Structures and functional properties of apple (*Malus domestica* Borkh) fruit starch. *Carbohydr. Polym.* **2006**, *63* (3), 432–441.
(32) Regina, A.; Bird, A.; Topping, D.; Bowden, S.; Freeman, J.; Barsby, T.; Kosar-Hashemi, B.; Li, Z. Y.; Rahman, S.; Morell, M. High-amylose wheat generated by RNA interference improves indices of large-bowel health in rats. *Proc. Natl. Acad. Sci. U.S.A.* **2006**, *103* (10), 3546–3551.
(33) Singh, N.; Singh, J.; Kaur, L.; Sodhi, N. S.; Gill, B. S. Morphological, thermal and rheological properties of starches from different botanical sources. *Food Chem.* **2003**, *81* (2), 219–231.
(34) Stevenson, D. G.; Yoo, S. H.; Hurst, P. L.; Jane, J. L. Structural and physicochemical characteristics of winter squash (*Cucurbita maxima* D.) fruit starches at harvest. *Carbohydr. Polym.* **2005**, *59* (2), 153–163.
(35) Kayisu, K.; Hood, L. F. Molecular-structure of banana starch. *J.f Food Sci.* **1981**, *46* (6), 1894–1897.
(36) Ling, L. H.; Fernandes, J. B.; Reilly, P. J.; Osman, E. M. Physical-properties of starch from Cavendish banana fruit. *Starke* **1982**, *34* (6), 184–188.
(37) Garcia, E.; Lajolo, F. M. Starch transformation during banana ripening—The amylase and glucosidase behavior. *J. Food Sci.* **1988**, *53* (4), 1181–1186.
(38) Zhang, P. Y.; Whistler, R. L.; BeMiller, J. N.; Hamaker, B. R. Banana starch: production, physicochernical properties, and digestibility—A review. *Carbohydr. Polym.* **2005**, *59* (4), 443–458.
(39) Nodaa, T.; Kottearachchib, N. S.; Shogo Tsudaa, M. M.; Takigawaa, S.; Matsuura-Endoa, C.; Kima, S.-J.; Yamauchia, N. H. a. H. Starch phosphorus content in potato (*Solanum tuberosum* L.) cultivars and its effect on other starch properties. *Carbohydr. Polym.* **2006**, *68* (4), 793–796.
(40) Kasemsuwan, T.; Jane, J. L. Quantitative method for the survey of starch phosphate derivatives and starch phospholipids by P-31 nuclear magnetic resonance spectroscopy. *Cereal Chem.* **1996**, *73* (6), 702–707.
(41) Stevenson, D. G.; Doorenbos, R. K.; Jane, J. L.; Inglett, G. E. Structures and functional properties of starch from seeds of three soybean (*Glycine max* (L.) Merr.) varieties. *Starch-Starke* **2006**, *58* (10), 509–519.
(42) Cooke, D.; Gidley, M. J. Loss of crystalline and molecular order during starch gelatinization—Origin of the enthalpic transition. *Carbohydr. Res.* **1992**, *227*, 103–112.
(43) Simao, R. A.; Silva, A. P. F. B.; Peroni, F. H. G.; do Nascimento, J. R. O.; Louro, R. P.; Lajolo, F. M.; Cordenunsi, B. R. Mango starch degradation. I. A microscopic view of the granule during ripening. *J. Agric. Food Chem.* **2008**, *56* (16), 7410–7415.
(44) Fujita, S.; Yamamoto, H.; Sugimoto, Y.; Morita, N.; Yamamori, M. Thermal and crystalline properties of waxy wheat (*Triticum aestivum* L.) starch. *J. Cereal Sci.* **1998**, *27* (1), 1–5.
(45) Zhong, F.; Yokoyama, W.; Wang, Q.; Shoemaker, C. F. Rice starch, amylopectin, and amylose: Molecular weight and solubility in dimethyl sulfoxide-based solvents. *J. Agric. Food Chem.* **2006**, *54* (6), 2320–2326.
(46) You, S.; Stevenson, S. G.; Izydorczyk, M. S.; Preston, K. R. Separation and characterization of barley starch polymers by a flow field-flow fractionation technique in combination with multiangle light scattering and differential refractive index detection. *Cereal Chem.* **2002**, *79* (5), 624–630.
(47) Yoo, S. H.; Jane, J. L. Molecular weights and gyration radii of amylopectins determined by high-performance size-exclusion chromatography equipped with multi-angle laser-light scattering and refractive index detectors. *Carbohydr. Polym.* **2002**, *49* (3), 307–314.
(48) Hizukuri, S. Polymodal distribution of the chain lengths of amylopectins, and its significance. *Carbohydr. Res.* **1986**, *147* (2), 342–347.
(49) Gidley, M. J.; Eggleston, G.; Morris, E. R. Selective removal of alpha-D-galactose side-chains from rhizobium capsular polysaccharide by guar alpha-D-galactosidase—Effect on conformational stability and gelation. *Carbohydr. Res.* **1992**, *231*, 185–196.

(50) You, S.; Izydorczyk, M. S. Molecular characteristics of barley starches with variable amylose content. *Carbohydr. Polym.* **2002**, *49*, 33–42.
(51) Baxter, C. J.; Carrari, F.; Bauke, A.; Overy, S.; Hill, S. A.; Quick, P. W.; Fernie, A. R.; Sweetlove, L. J. Fruit carbohydrate metabolism in an introgression line of tomato with increased fruit soluble solids. *Plant Cell Physiol.* **2005**, *46* (3), 425–437.
(52) Robinson, N. L.; Hewitt, J. D.; Bennett, A. B. Sink metabolism in tomato fruit. 1. Developmental-changes in carbohydrate metabolizing enzymes. *Plant Physiol.* **1988**, *87* (3), 727–730.
(53) MuForster, C.; Huang, R. M.; Powers, J. R.; Harriman, R. W.; Knight, M.; Singletary, G. W.; Keeling, P. L.; Wasserman, B. P. Physical association of starch biosynthetic enzymes with starch granules of maize endosperm—Granule-associated forms of starch synthase I and starch branching enzyme II. *Plant Physiol.* **1996**, *111* (3), 821–829.
(54) Boren, M.; Larsson, H.; Falk, A.; Jansson, C. The barley starch granule proteome—Internalized granule polypeptides of the mature endosperm. *Plant Sci.* **2004**, *166* (3), 617–626.
(55) Rahman, S.; Kosarhashemi, B.; Samuel, M. S.; Hill, A.; Abbott, D. C.; Skerritt, J. H.; Preiss, J.; Appels, R.; Morell, M. K. The major proteins of wheat endosperm starch granules. *Aust. J. Plant Physiol.* **1995**, *22* (5), 793–803.
(56) Craig, J.; Lloyd, J. R.; Tomlinson, K.; Barber, L.; Edwards, A.; Wang, T. L.; Martin, C.; Hedley, C. L.; Smith, A. M. Mutations in the gene encoding starch synthase II profoundly alter amylopectin structure in pea embryos. *Plant Cell* **1998**, *10* (3), 413–426.
(57) Smith, A. M.; Quintontulloch, J.; Denyer, K. Characteristics of plastids responsible for starch synthesis in developing pea embryos. *Planta* **1990**, *180* (4), 517–523.
(58) Smith, A. M. Evidence that the waxy protein of pea (*Pisum sativ*um L.) is not the major starch-granule-bound starch synthase. *Planta* **1990**, *182* (4), 599–604.
(59) Dian, W. M.; Jiang, H. W.; Chen, Q. S.; Liu, F. Y.; Wu, P. Cloning and characterization of the granule-bound starch synthase II gene in rice: gene expression is regulated by the nitrogen level, sugar and circadian rhythm. *Planta* **2003**, *218* (2), 261–268.

Received for review July 7, 2008. Revised manuscript received October 19, 2008. Accepted October 26, 2008. We thank the Anandamahidol Foundation, which provided financial support to K.L. This work was funded by National Science Foundation Grant MCB-0620001 (D.M.B.).

JF802064W